Article Identifier
DOI: 10.22032/dbt.58840
URN: urn:nbn:de:gbv:ilm1-2023isc-108:6

AEROSTATIC PUMP SEAL

Onni Leutonen, Petteri Haverinen, Valtteri Vainio, Mikael Miettinen, Jaakko Majuri, Raine Viitala

Mechatronics Group, Aalto University, Espoo, Finland

ABSTRACT

Process pumps commonly utilize water-lubricated mechanical face seals. The seal faces are commonly silicon carbide or other durable materials. However, the reliance on water flush for the lubrication of the seal poses challenges due to wear. The wear is result of abrasive particles and corrosion problems originating from the leaking water. To address these issues, this paper investigates the feasibility of an aerostatic seal system. The proposed seal comprises two aerostatic seals mounted to a pressure-fed chamber: one facing the pump chamber and the other facing the ambient. Both of the sealing surfaces are flexibly supported and preloaded against the seals. A chamber between the seals is pressurized, which causes flow through the air gaps of the seals towards the ambient and the pump chamber. The flow prevents pump chamber liquid from leaking into, and through the seal. Thus, only seal supply gas is exhausted to the ambient. The feasibility of the seal concept was validated experimentally. The seal air consumption, leakage, and pressures in various parts of the system were measured. The application of this type of seal in the paper industry, particularly for pumping cellulose-liquid mixtures using centrifugal pumps, could reduce the frequency of seal replacements and eliminate water leakage.

Index Terms - aerostatic seal, pump seal, face seal, tribology, porous gas elements, thin-film lubrication.

1. INTRODUCTION

Centrifugal process pumps are commonly used in the industry for pumping large volumes of liquids, that may even contain gases and solids within [1]. The fluid flows into the pump along the rotational axis of the impeller. The rotation of the impeller forces the fluid to flow through the impeller vanes against the volute pump casing. The volute chamber increases in cross-sectional area towards the outlet of the pump creating pressure difference and therefore flow towards the outlet.

The shaft of the impeller must be sealed to the housing to prevent fluid leakage from the pump chamber, which is commonly accomplished with high-precision water lubricated mechanical face seals [2]. The seal elements require high wear resistance. Commonly, the seal system consists of a pair of back-to-back annular silicon carbide seal faces with pressurized water filled seal chamber between them. The high pressure is used to force flow out of both seals, into the process side and into the ambient. The water supply lubricates the face seals, flushes contaminants away from the seal gap and stops leakage from the process to the ambient. In each pair of the seal faces, one face rotates with the shaft and the other is fixed to the pump body. Both faces are flexibly supported to overcome any alignment errors [2].

The pressure of the seal chamber is set higher than the pressure in the pump chamber in the immediate vicinity of the seal. The pressure difference between seal chamber and pump chamber causes water flow through the seal gap towards the pump chamber. Correspondingly, the pressure difference between seal chamber and the ambient causes water leakage through the second seal gap towards the ambient. The water leakage is required for the lubrication of the sealing surfaces, but it causes contamination of the process liquid and leakage to outside of the pump casing.

In the present study, a novel sealing system based on an aerostatic seal was investigated. A porous aerostatic bearing was adapted to create an aerostatic seal. The aerostatic sealing system was designed to directly replace commonly used water lubricated mechanical sealing system. The investigated seal was an annular porous aerostatic face seal. The principles of the design were analogous to the mechanical seal, two back-to-back seals were used to divide a chamber, that was fed with pressurized air. The aerostatic seal system was designed to fit into the dimensions of the typical mechanical face seals, thus being able to serve as a drop-in replacement. Advantages of the proposed seal include replacing water leakage with air leakage reducing plumbing requirements and causes of corrosion.

Aerostatic seals are based on aerostatic bearings. Aerostatic bearing creates its load carrying capacity with externally supplied pressurized gas, often air. The supplied gas is distributed to the bearing surface with a restrictor creating a thin high-pressure gas film in the bearing clearance. Aerostatic bearings with porous restrictors have relatively high stiffness, load carrying capacity and stability compared to other restrictor types due to uniform pressure profile in the bearing clearance [3]. The high-pressure gas film allows the bearing to be used as a seal [4].

The investigated seal system was validated experimentally using a test setup. The test setup consisted of a prototype seal unit, centrifugal pump housing and a drive motor. No impeller was used to negate any effects of the pumping action on the seal. The pump chamber was filled with water and pressurized pneumatically to simulate the operating conditions of the pump. The operating pressures and flows of the seal chamber, pump chamber and aerostatic seals were measured. The results were used to validate the feasibility of the seal concept, and the performance of the prototype seal.

2. METHODS

2.1 Prototype seal design

The investigated two-stage aerostatic sealing system has two seals with a pressurized chamber between them. The pressure of the seal chamber is set higher than the pressure in the pump chamber in the immediate proximity of the seal. The intermediate pressurized volume limits the pressure difference over a seal and allows for the thrust loads of the two seals to counteract each other. The ambient seal limits the air leakage to the atmosphere from the seal chamber. In normal operating conditions, the pressure difference over the ambient side is relatively high compared to the pressure difference over the pump chamber side seal, resulting in higher flow from seal chamber to ambient. However, the seal chamber can also be supplied at lower pressure than that of the pump chamber. In such situation the supply pressure of the seal elements should be sufficiently high to provide flow into the seal chamber and pump chamber as presented in Table 2.

The aerostatic seal element consists of a seal body and porous graphite restrictor. The seal body has a supply groove that distributes pressurized air behind the graphite restrictor. The graphite restrictor is attached to the bearing body with epoxy adhesive. The seal body on the pump chamber side is rigidly attached to the pump body while the seal body on the ambient side is mounted axially free to the housing and preloaded against the seal surface. Flexible support of both seal surfaces and the ambient seal body is achieved with rubber O-rings that also seal the seal chamber from the pump chamber and the ambient. The flexible support negates the effects of alignment errors and allows the pump chamber seal surface and the ambient seal body to move axially to adjust the seal clearance. Preload is applied to pump chamber seal surface and ambient seal body with wave springs. The components of the seal system assembly are presented in Figure 1.

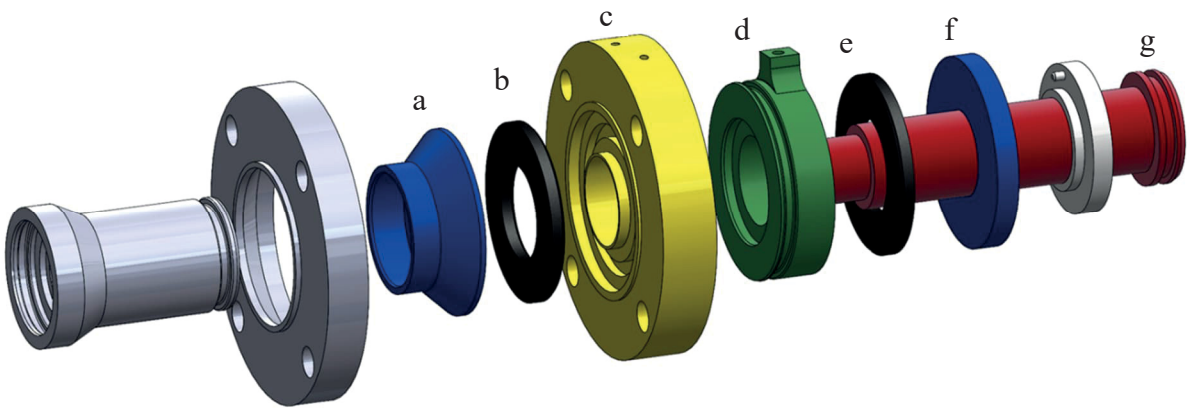

Figure 1. Exploded view of the aerostatic pump seal assembly. a) Pump chamber seal surface. b) Pump chamber side seal restrictor. c) Pump chamber side seal body. d) Ambient seal body. e) Ambient seal restrictor. f) Ambient seal surface. g) Pump shaft.

The average pressure in the seal clearance is estimated to be half of the input pressure [5]. Therefore, seal input pressure is multiplied with factor $k = 0.5$ to calculate estimated average pressure in the seal clearance. The forces caused by the preload springs are neglected, as they are negligible compared to the pressure forces. The main dimensions related to the surface areas relevant to the pressure forces are presented in Table 1. Figure 2 presents a cross section of the seal system with the main functional dimensions of the seal elements.

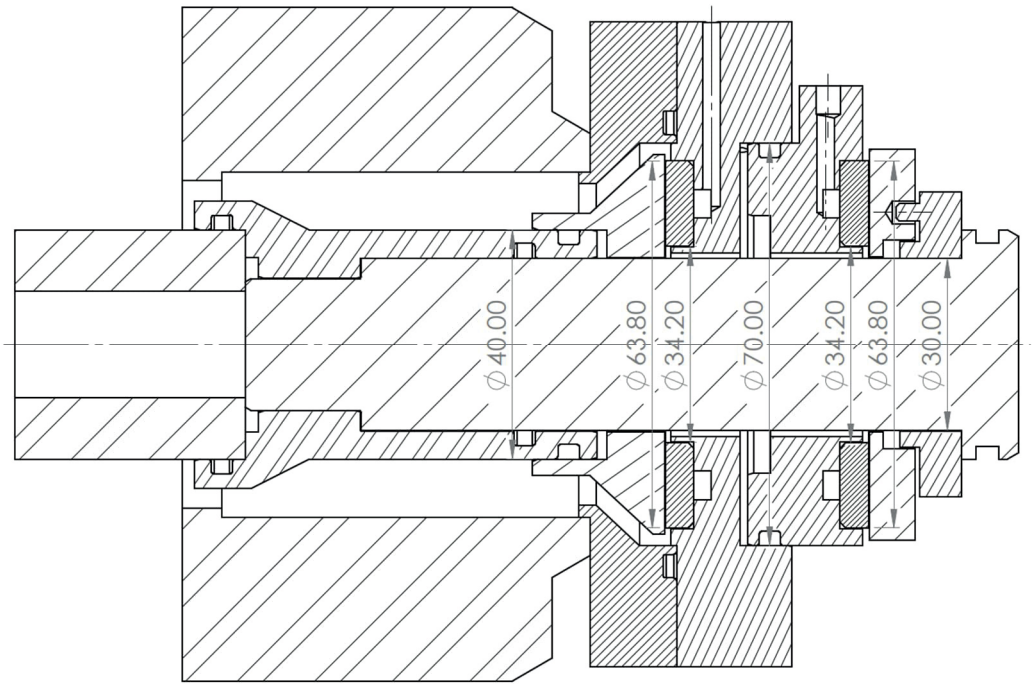

Figure 2. Cross-section of seal system with dimensions used for surface area calculations.

Table 1. Dimensions used for surface area calculations.

Dimension	Description	Value (mm)
$d_{ss.pc}$	Pump chamber seal surface, pump chamber side inner diameter	40.0
$D_{ss.pc}$	Pump chamber seal surface, pump chamber side outer diameter	63.8
$d_{ss.sc}$	Pump chamber seal surface, seal chamber side inner diameter	34.2
$D_{ss.sc}$	Pump chamber seal surface, seal chamber side outer diameter	40.0
$d_{sb.sc}$	Ambient seal body, seal chamber side inner diameter	34.2
$D_{sb.sc}$	Ambient seal body, seal chamber side outer diameter	70.0
d_g	Porous graphite restrictor inner diameter	34.2
D_g	Porous graphite restrictor outer diameter	63.8

Effective surface area of pump chamber pressure P_{pc} on the pump chamber seal surface:

$$A_{ss.pc} = \frac{\pi}{4}\left(D_{ss.pc}^2 - d_{ss.pc}^2\right) \quad (1)$$

Effective surface area of seal chamber pressure P_{sc} on the pump chamber seal surface:

$$A_{ss.sc} = \frac{\pi}{4}\left(D_{ss.sc}^2 - d_{ss.sc}^2\right) \quad (2)$$

Effective surface area of seal chamber pressure P_{sc} on the ambient seal body:

$$A_{sb.sc} = \frac{\pi}{4}\left(D_{sb.sc}^2 - d_{sb.sc}^2\right) \quad (3)$$

Surface area of the seal face, i.e., the surface area of the porous graphite restrictor:

$$A_g = \frac{\pi}{4}(D_g^2 - d_g^2)$$

(4)

The maximum pressure of the pump chamber was determined by calculating the forces on the individual aerostatic seals. The equations for load calculations are presented in Equations 7 and 8. The maximum load carry capacity for the pump chamber seal and ambient seal are presented in equations 5 and 6.

The maximum load carry capacity for the pump chamber seal F_{psmax}:

$$F_{psmax} = A_g P_{pcs} k$$

(5)

The maximum load carry capacity for the ambient seal F_{asmax}:

$$F_{asmax} = A_g P_{es} k$$

(6)

The total load on the pump chamber seal surface F_{ss}:

$$F_{ss} = A_{ss.pc} P_{pc} + A_{ss.sc} P_{sc}$$

(7)

The total load on the ambient seal body F_{sb}:

$$F_{sb} = A_{sb.sc} P_{sc}$$

(8)

The bearing clearance is above zero when the maximum carry capacity of a seal is more than the total load acting on the pump chamber seal surface and the ambient seal body:

$$F_{psmax} > F_{ss} \quad \& \quad F_{asmax} > F_{sb}$$

(9)

The forces on pump chamber seal surface and ambient seal body at different pump and seal chamber pressures are presented in Figure 3. The touchdown of either the pump chamber seal or the ambient seal limits the maximum pressure of the pump chamber. Aerostatic seal touchdown occurs when the total force acting on floating seal elements is greater than the maximum load capacity of the seal. The maximum pump chamber pressure is presented in Figure 3, as the intersection point between the maximum load capacity and seal element forces.

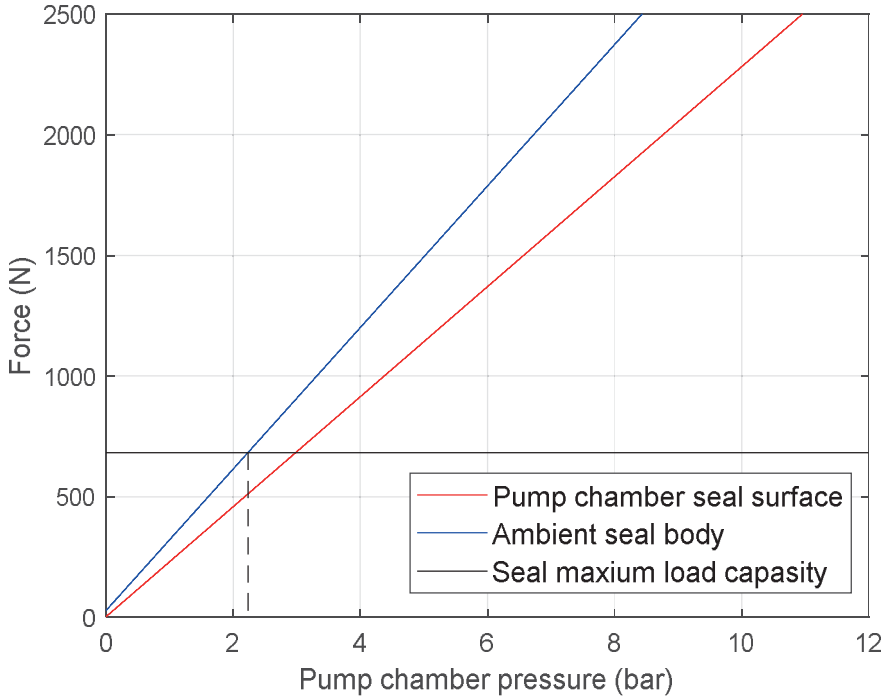

Figure 3. Linear approximation of load on pump chamber seal surface and ambient seal body and seal load carrying capacity at pump chamber pressures from 0 MPa to 12 MPa. The seal chamber pressure is at 0.01 MPa over the pump chamber pressure. Input pressures of both seals is 0.6 MPa. The vertical dashed line illustrates the maximum theoretical pressure of the pump chamber before seal touchdown.

2.3 Test setup

The test setup consisted of the industrial pump unit where the seal was replaced with aerostatic pump seal. The system included also pneumatic and electrical measuring and control system. The aerostatic seal was mounted on a process pump, which was driven by a 3-phase motor. The impeller was removed prior to testing to allow the testing of the system without pumping liquid, thus eliminating the need for a hydraulic system. The system included pneumatic and electrical measuring and controlling system.

The pump chamber, seal chamber and both aerostatic seals were pressurized externally via the pneumatic system. The chamber was filled with water to simulate the process liquid. The control parameters for the test setup were angular velocity of the motor and the pressures of the seal chamber, pump chamber and seal elements. In figure 4 the construction of the test setup is presented. The bearings were housed inside of the pump housing next to the seal unit.

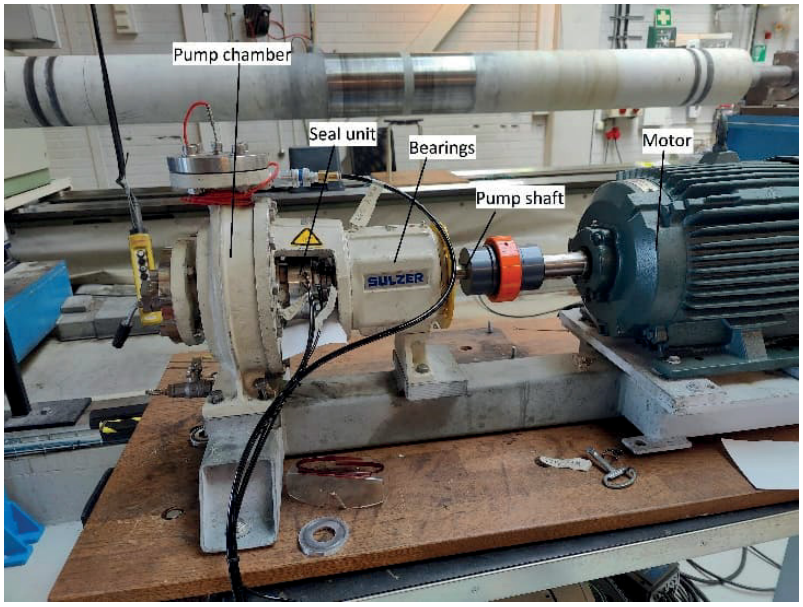

Figure 4. Test setup. From left to right: Pump chamber and seal unit mounted on a pump housing, pump shaft bearings, pump shaft and motor.

2.4 Pneumatic system

The pneumatic system was designed to control the pressures in the pump and seal chambers and adjust the feed pressures into the aerostatic sealing elements, as described in chapter 2.3. The flow and pressure from each of the chambers and seal elements were measured using flow and pressure sensors mounted to each air supply line. The system supply pressure was 0.65 MPa meanwhile the operating pressures for the seal elements were 0.6 MPa. The graphite seal elements were modelled as restrictors as seen in Figure 5. The air gaps created by the seal elements are represented as variable restrictors since the amount of flow through the air gap is governed by the height of the air gap. Air gap is present in the seal clearance.

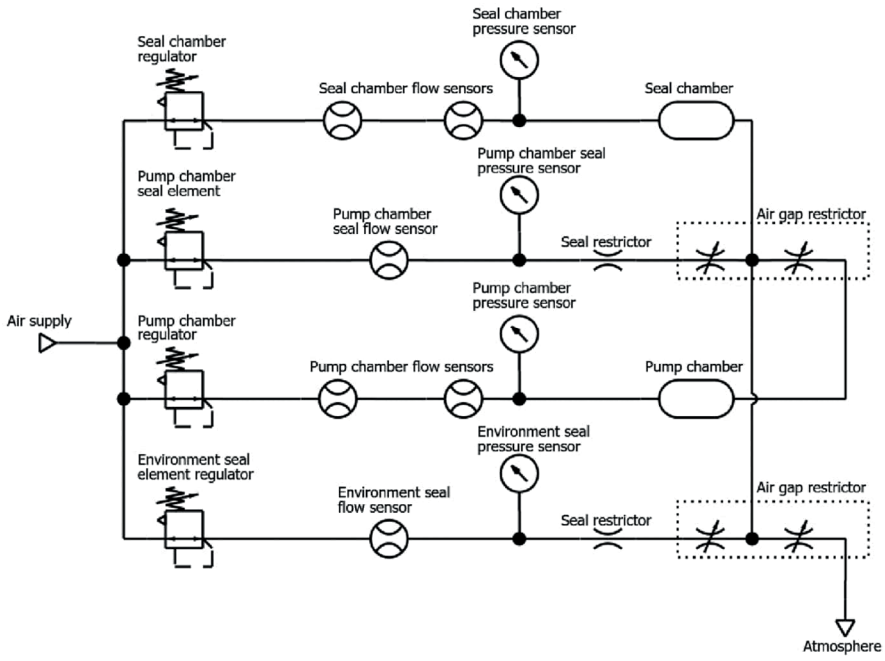

Figure 5. Pneumatic diagram. Seal restrictors depict the graphite in the seal elements. Air gap restrictors depict the air gaps, which cause resistance to flow depending on the air gap height.

The air supply was directed to each seal elements, seal chamber and pump chamber. The flow of the pump and seal chambers was measured with two flow sensors connected in series since the chambers can flow in both directions depending on the pressure difference between the pump chamber and seal chamber. Table 2 represents the possible flow directions. The flow direction under normal operation conditions ($P_{sc} > P_{pc}$) is from the seal chamber to pump chamber and from seal chamber to ambient. The flow is restricted from the seal chamber to pump chamber through pump seal air gap. The flow from seal chamber to ambient is restricted respectively by the air gap of the ambient seal element. The seal elements can cause flow to the seal chamber, which may cause flow out of both the seal chamber and pump chamber, when the pressure difference is near zero. The flows out of the seal elements are always greater than or equal to zero.

Table 2. Flow direction in relation to pressure difference between P_{sc} and P_{pc}, where P_{sc} is the seal chamber pressure and P_{pc} is the pump chamber pressure.

Pressure difference	Seal chamber	Pump chamber
$P_{sc} > P_{pc}$	IN	OUT
$P_{sc} \cong P_{pc}$	OUT	OUT
$P_{sc} < P_{pc}$	OUT	IN

2.5 Electrical system

To control the regulators and motor and to measure flow and pressure, an electrical system was designed. It was integrated with the pneumatic system in one electrical cabinet. The signals from the sensors were converted from analogue to digital values using NI-9205 analogue-to-digital converter (ADC). The control signals for the motor controller and regulators were converted from digital signals from pc to analogue values using NI-9264 digital-to-analogue converter (DAC). Both the ADC and DAC have resolution of 16 bits and sample rate of 100 kHz. The interface from the electrical system to the measurement PC was made with LabView.

Table 3. Sensors used in the measurement setup.

Device	Type	Application	Range	Accuracy (FMS)
Pressure sensor	SMC PSE540	Chambers, seals	0 – 1.0 MPa	2%
Flow sensor	SMC PFM750	Seal chamber inflow, pump chamber outflow	1 - 50 l/min	1%
Flow sensor	SMC PF2M710	Seal chamber outflow, pump chamber inflow	0.1 - 10 l/min	1%
Flow sensor	SMC PFM710	Seal elements	0.2 - 10 l/min	1%
Pressure regulator	SMC ITV1050	Chambers, seals	0.005 - 0.9 MPa	1%

2.6 Procedure of experiments

Preparation of the test setup was as follows: The seal chamber was first pressurized with 0.1 MPa. Water was added to the pump chamber to act as the process liquid. The aerostatic seal elements were pressurized to 0.6 MPa and the pump chamber closed. The pump chamber was then pressurized to 0.09 MPa.

The analytical approximation demonstrated maximum pump chamber pressure at 0.22 MPa. Therefore, the pressure range was selected to be from 0.1 MPa to 0.2 MPa at 0.025 MPa intervals with 0.01 MPa pressure difference between the seal chamber and pump chamber. The seal chamber was constantly at higher pressure than the pump chamber.

The pressures of the pump chamber and seal chamber were increased in each measurement by 0.025 MPa while the aerostatic seal elements were kept at constant 0.6 MPa. The pump motor was then run for 10 minutes at 4.85 Hz. The complete procedure is seen in Figure 6.

The leakage to ambient Q_{amb} was calculated as a sum of the flows in and out of the seal:

$$Q_{amb} = Q_{sc} + Q_{ps} + Q_{as} - Q_{pc} \quad (10)$$

Where Q_{sc} is flow into the process chamber , Q_{ps} is flow into the pump seal element, Q_{as} is flow into the ambient seal element and Q_{pc} is flow out of the pump chamber.

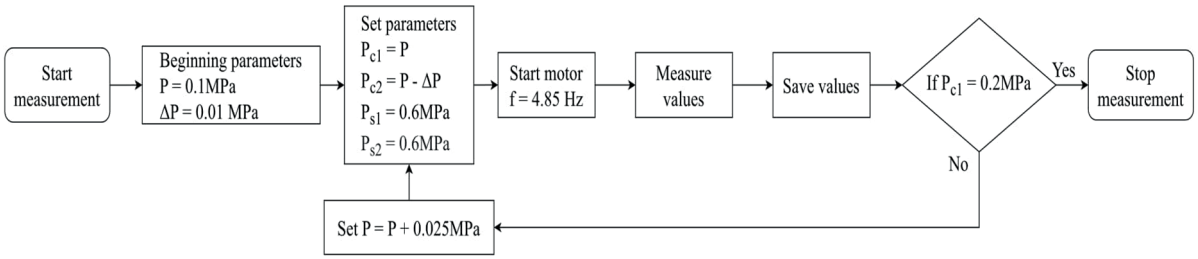

Figure 6. Flow chart of the experiment procedure, where P_{c1} is the seal chamber pressure, P_{c2} is the pump chamber pressure, P_{s1} is pump chamber side aerostatic seal pressure, P_{s2} is seal chamber side aerostatic seal pressure and ΔP is the pressure difference over the seal. The pressure parameters are supply parameters, which is why they use different notations from the measuring.

3. RESULTS

Measurements were made with seal chamber pressure between 0.1 MPa and 0.2 Mpa and pump chamber pressure between 0.09 MPa and 0.19 MPa. During the measurements, the supply pressure to both seal elements was 0.6 MPa.

Flow and leakage into the pump chamber and ambient is presented in Figure 7. Flow into the seal elements is presented in Figure 8. During testing possible water leaks were monitored visually and no leaks were detected. The supply air consumption was 13.6 l/min at maximum and stabilized to 10 l/min after the seal chamber reached 0.15 MPa.

In Figures 7 and 8 the flows are presented as a function of pressure. The seal chamber flow was constantly positive while the pump chamber flow was constantly negative. From Figures 7 and 8 the flow in each of the chambers and to ambient was decreasing when the pressure was increased. An equilibrium point was reached at seal chamber pressure of 0.15 MPa.

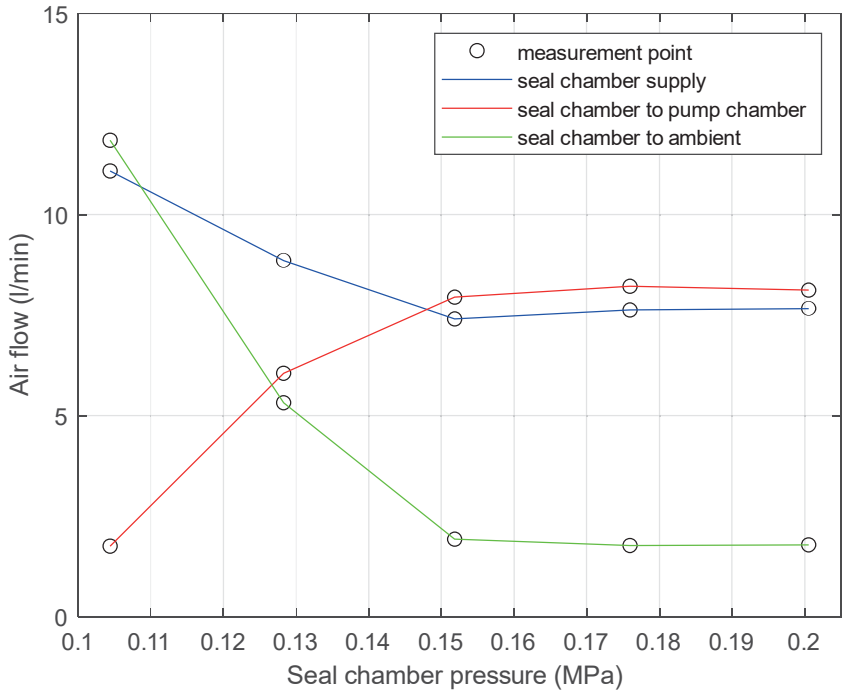

Figure 7. Air flow vs seal chamber pressure. Dots are measuring points, green line is air leakage to ambient, red is flow from seal chamber to pump chamber, and blue is flow to seal chamber.

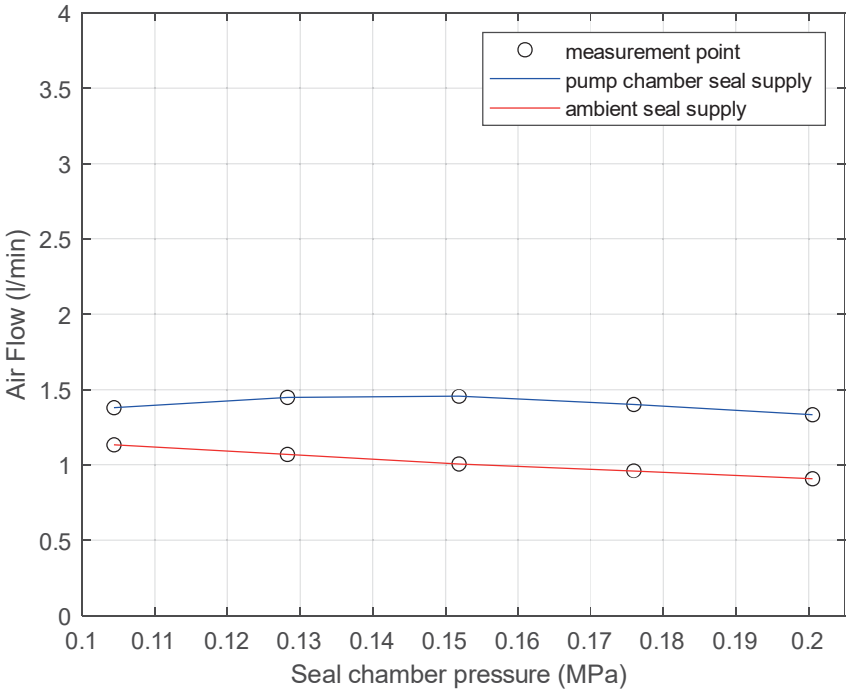

Figure 8. Air flow vs seal chamber pressure. Dots are measuring points, blue line is flow through the pump chamber seal element, red line is flow through the ambient seal element.

4. DISCUSSION

Presented results suggest that the seal system was sealing the pump chamber from ambient in the measurements. This was determined based on the direction of the flow. The flow direction was constantly from the seal chamber to the pump chamber, which means there was no flow from the pump chamber to the seal chamber. Reaffirming this result was the observation of no detectable water leaks and no water in seal chamber after disassembly of the seal unit.

The seal elements, especially the ambient seal (Figure 8), had a slight decrease in flow as the pressure in the seal chamber was increased. This was expected since the increased load decreases the height of the air gap, which increases the flow restriction of the air gap. The increased flow restriction then decreased the flow through the seal elements.

The current seal design has an estimated maximum seal chamber pressure of 0.22 MPa. The load capacity of the ambient seal limits the maximum operating pressure of the pump seal. By decreasing the surface area, where the seal chamber pressure can affect the ambient seal body, the pressure of seal and pump chamber can be increased without ambient seal touchdown. In addition, the load carrying capacity of the pump chamber seal limits the operating pressure to a maximum of 0.30 MPa. Figure 9 illustrates the forces on pump chamber seal surface and ambient seal body at different pump and seal chamber pressures with reduced effective surface area of the ambient seal body. The increase of the input pressure of the aerostatic seals is necessary to reach higher pump chamber pressures as seen in Figure 10.

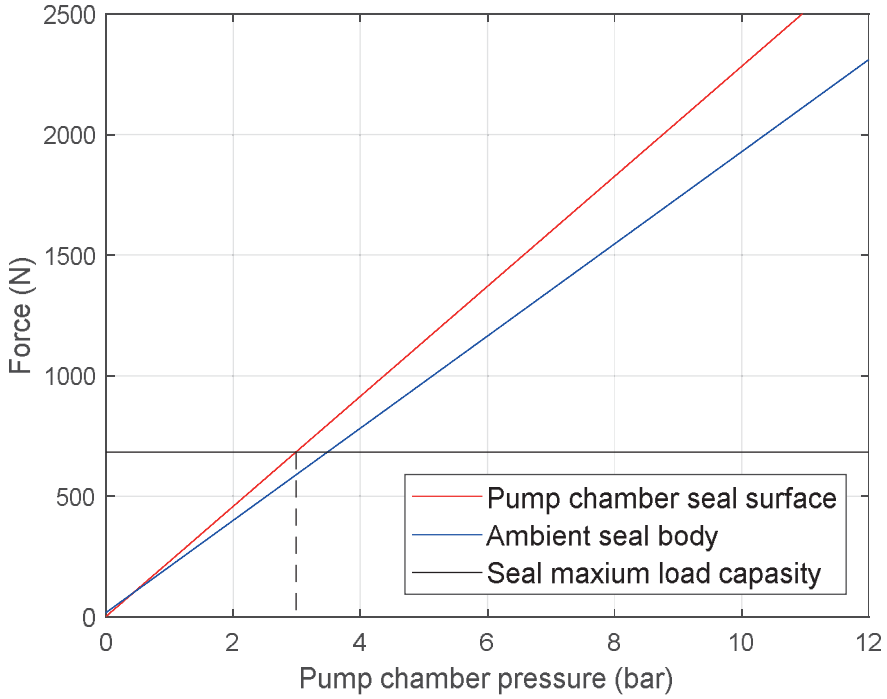

Figure 9. linear approximation of load on pump chamber seal surface and ambient seal body and seal load carrying capacity at pump chamber pressures from 0 MPa to 12 MPa. The ambient seal body, seal chamber side outer diameter $D_{sb.sc}$ is decreased by 10 mm. The seal chamber pressure is at 0.01 MPa over the pump chamber pressure. Input pressure of both seals is 0.6 MPa. The vertical dashed line illustrates the maximum theoretical pressure of the pump chamber before seal touchdown.

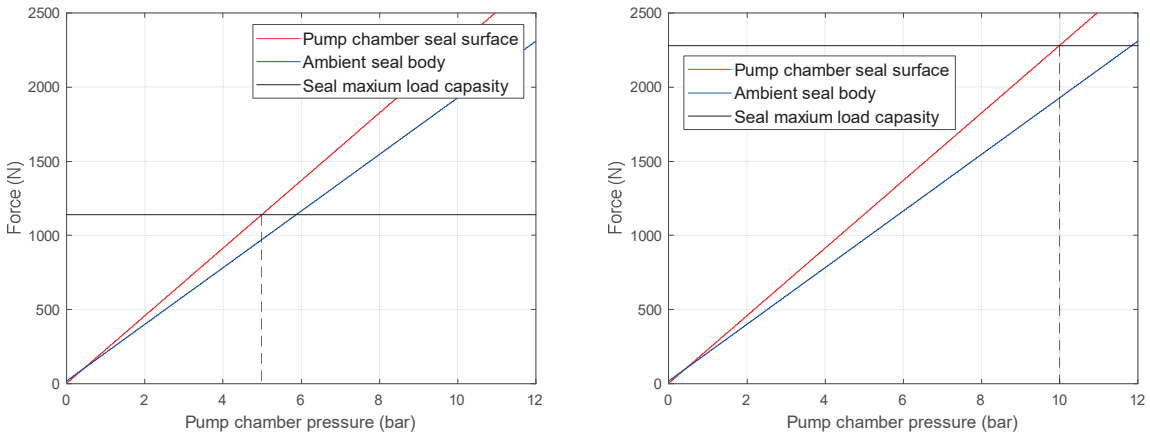

Figure 10. Linear approximation of load on pump chamber seal surface and ambient seal body and seal load carrying capacity at pump chamber pressures from 0 MPa to 12 MPa. The ambient seal body, seal chamber side outer diameter $D_{sb.sc}$ is decreased by 10 mm. The seal chamber pressure is 0.01 MPa over the pump chamber pressure. Input pressure of seals is constant (a) 1.0 MPa and (b) 2.0 MPa. The vertical dashed line illustrates the maximum theoretical pressure of the pump chamber before seal touchdown.

5. CONCLUSION

The present study developed and experimentally verified the feasibility of a novel aerostatic seal. The seal consisted of two porous aerostatic graphite seals connected to a central seal chamber. The seal chamber and pump chamber had a constant pressure difference of 0.01 MPa, with seal chamber being kept at a higher pressure. The aerostatic seal elements were kept at constant pressure of 0.6 MPa. The pressure difference caused flow into the pump chamber. The direction and volume of air flow was measured to determine the performance of the seal. The total air consumption of the system was reasonable reaching maximum of 13.6 l/min and settling to 10 l/min after equilibrium point was reached.

The seal performed well in the tested seal chamber pressure range of 0.09 MPa to 0.2 MPa. However, industrial applications require preferably at least 1.0 MPa pump chamber operating pressure. Thus, further work will focus on optimizing the geometry of the seal to be able to reach the higher operating pressures required. The wear of the graphite restrictors in the seal elements was undetermined and will be the scope of a future research.

REFERENCES

[1] J. F. Gülich, Centrifugal pumps, Cham, Switzerland: Springer, 2020.

[2] J. Netzel, “Mechanical Seals,” in *Encyclopedia of Tribology*, Boston, Springer, 2013, pp. 2209-2218.

[3] Q. Gao, W. Chen, L. Lu, D. Huo and K. Cheng, “Aerostatic bearings design and analysis with the application to precision engineering: State-of-the-art and future perspectives,” *Tribology International,* vol. 135, pp. 1-17, 2019.

[4] J. Wilhelm, C. Schwitzke, H.-J. Bauer and T. Nquyen, “A new approach for scaling aspirating face seal aerodynamics,” *Journal of Engineering for Gas Turbines and Power,* vol. 141, no. 3, 2018.

[5] New Way Air Bearings, “Air bearing application and design guide,” January 2006. [Online]. Available: https://www.newwayairbearings.com/sites/default/files/new_way_application_and_design_guide_%20Rev_E_2006-01-18.pdf. [Accessed June 2023].

CONTACTS

O. Leutonen email: onni.leutonen@aalto.fi

P. Haverinen email: petteri.haverinen@aalto.fi

V. Vainio email: mikael.miettinen@aalto.fi

M. Miettinen email: valtteri.s.vainio@aalto.fi

J. Majuri email: jaakko.majuri@aalto.fi

R. Viitala email: raine.viitala@aalto.fi

